DD

Institut
de Physique
Nucléaire
de Lyon

Université Claude Bernard

IN2P3 - CNRS

LYCEN 9613
CMS TN / 96-052
Juin 1996

Investigation of avalanche photodiodes

D. Si Mohand, Y. Benhammou, P. Depasse, M. Goyot,
B. Ille, E. Linard, F. Martin, Y. Musienko[1]

Institut de Physique Nucléaire de Lyon, IN2P3/CNRS, Université Claude Bernard,
F-69622 Villeurbanne Cedex, France

[1]*I.N.R. Moscow, Russia*

43, Boulevard du 11 Novembre 1918 - 69622 VILLEURBANNE Cedex - France

CMS TN/ 96-052
June 5, 1996

Investigation of Avalanche Photodiodes

D. Si Mohand, Y. Benhammou, P. Depasse, M. Goyot,
B. Ille, E. Linard, F. Martin, Y. Musienko [1]
Institut de physique nucléaire, Lyon, France

Abstract

Some characteristics and performances of a set of nine Hamamatsu avalanche photodiodes have been investigated. These APDs have equipped a small 3x3 $PbWO_4$ crystal matrix in X3 beam during the summer of 1995. This note summarizes the main results of this work.

[1] On leave from I.N.R., Moscow, Russia

1 Introduction

An electromagnetic calorimeter with a high resolution is necessary to search for the Higgs if it has a mass between 80 and 160 GeV [1]. A $PbWO_4$ crystal option has been chosen by the CMS collaboration to achieve this task. The light is collected and converted into an electric charge by an Avalanche Photodiode (APD) followed by a fast preamplifier. The advantage of the APDs is that they are not sensitive to the strong magnetic field when compared to photomultipliers and they have a small nuclear counter effect when compared to PIN diodes.

In this study, we have tested nine low capacitance Hamamatsu APDs (S5345) received in spring, 1995 with an area of 0.2 cm^2. We have measured the capacitance and dark current for each APD. The gain measurements have also been done with gamma sources, continuous and pulsed light. The gain sensitivity versus bias and temperature have also been investigated succinctly.

2 Measurements of capacitance of APDs

An automatic capacitance bridge has been used to measure the capacitance of these nine APDs versus bias voltage.

Figure 1 shows an example of typical behaviour of the capacitance as a function of bias voltage. This behaviour suggests a complex intrinsic structure of the APD. The full depletion starts only at around 200 V, with the measured capacitance being 90 pF. From the point of view of noise, this is a rather high value but still reasonable for a fast shaping at LHC [2].

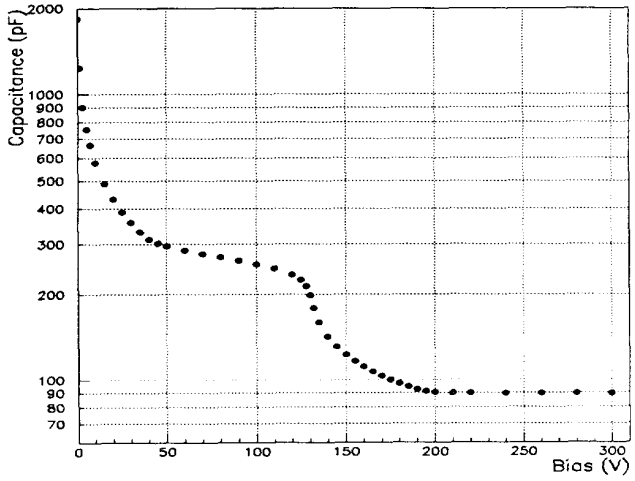

Figure 1: Capacitance of one Hamamatsu APD versus bias voltage.

3 Measurements of dark current of the APDs

The APD dark current is the sum of two contributions as presented in the equation:

$$I_d = I_s + I_b\, G$$

with:

- I_s as the surface leakage current which is proportional to the bias and is not affected by the multiplication process.
- I_b as the bulk leakage current which is affected by the multiplication process G.

This leakage current is measured directly by a Keithley 480 picoammeter for each bias voltage after having shielded and carefully isolated the APD from the light.

Figure 2 presents the results for the nine Hamamatsu APDs at a room temperature of 24.5 $°C$.

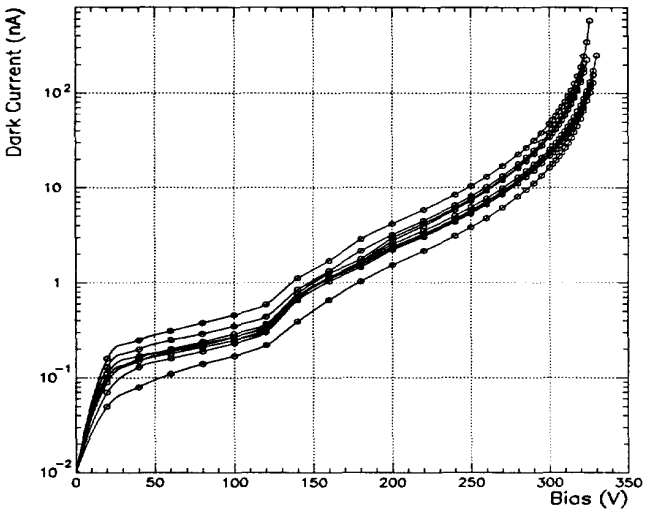

Figure 2: Dark current measurements of the Hamamatsu APDs 1995.

Thus at bias equalling 300 V the dark current I_d varies between 15 to 50 nA. This scattering in the leakage current values is due to the gain (G) dispersion of the APDs, see section 4.3, and the bulk current (I_b) dispersion, see section 4.6.

4 Continuous light method

4.1 Experimental set-up

Following the method described in reference [3], all of the Hamamatsu APDs have been exposed to a continuous blue light illumination, given off by a light emitting diode (LED) [4]. The LED intensity depends on the dc forward current supply of the diode. The light wavelength, $\lambda_d = 481$ nm, has been chosen in such a way as to have a total absorption in the entrance window before the gain region inside the APD. Indeed, if the light penetrates the gain region the measurements will be incorrect because part of the primary photoelectrons will exhibit smaller multiplication. The LED is placed approximately at 1 cm from the APD. The photocurrent has been measured by a Keithley 480 picoammeter for each bias voltage which is set with the Keithley 487/voltage source.

4.2 LED intensity effect on the photocurrent of the APD

In this section we have investigated a possible effect on the photocurrent measurements due to the LED intensity. We have recorded the photocurrent of Hamamatsu APD for four values of dc forward current 0.5, 1, 2 and 4 mA. These measurements have been taken with a temperature variation smaller than $0.5°C$.

The R_x ratio defined as:

$$R_x = \frac{Iph(x\ mA)}{Iph(0.5\ mA)}$$

is shown in figure 3 versus bias. Iph is the photocurrent of the APD measured with a LED forward current of x mA.

Assuming the LED intensity is proportional to the dc forward current, we expect the ratios R_4, R_2 and R_1 to be equal to 8, 4 and 2 respectively. If we don't take into account the results at high bias the predictions seem correct except for R_4 where the measured value is lower by 6%. This difference is due essentially to the non-linearity of the LED response to the dc forward current. This effect has been checked by using a PIN diode [2] and we found the ratio R_4 compatible with the value obtained in the case of the APD within 0.5%.

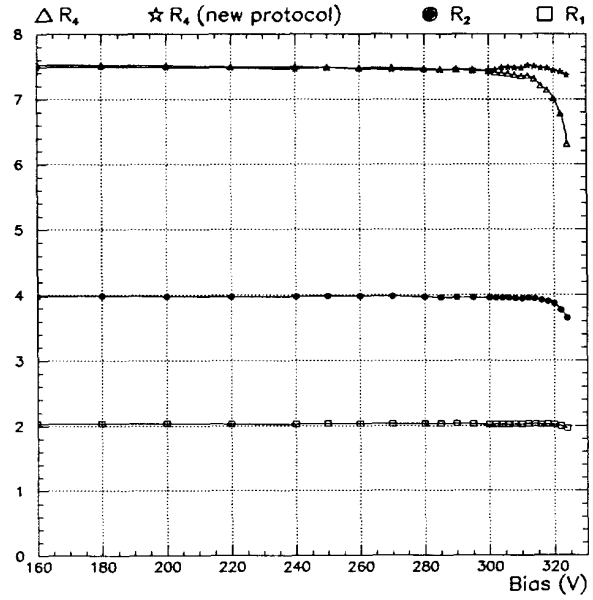

Figure 3: Normalised photocurrent of Hamamatsu APD versus bias.

From a particular bias threshold, dependent on the value of the dc forward current, the R_x ratio begins to decrease. Near the breakdown the relative decrease of the R_x ratio is around 8.5 and 16.5% for the dc forward current of 2 and 4 mA respectively.

This diminution of the ratio may be explained in two ways:

- increase of the temperature in the gain region due to a high photocurrent going through this region (high power to be dissipated).

[2] Hamamatsu S3590-01

- a hypothetical saturation phenomenon due to the high density of charge created in the avalanche region.

In order to discriminate between these two hypotheses, we have made another set of photocurrent measurements as a function of bias where the blue LED is now switched off for some time between two measurements. The value of the photocurrent is recorded immediately before it decreases. The star symbols in figure 3 show the ratio R_4 calculated from the photocurrent of the APD measured with this new procedure. The relative decrease of the ratio R_4 is now below 3% near the breakdown and it suggests that the difference observed at high bias is due essentially to the temperature effect.

Another way to check that the previous effect is not caused by a saturation effect is to plot (figure 4) the photocurrent of the APD as a function of PIN diode photocurrent by varying the dc forward current values from 0.5 to 21 mA. These measurements have been made with the new method and at three bias values of 300, 312 and 320 V.

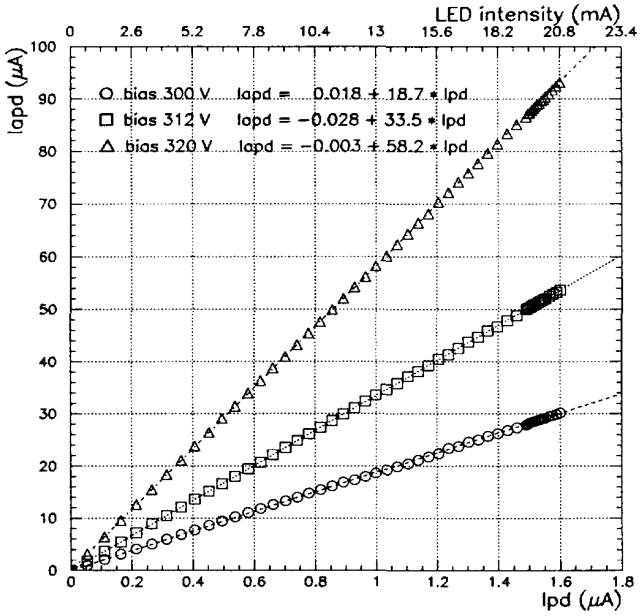

Figure 4: The APD photocurrent versus the PIN diode photocurrent for different values of the dc forward current of the LED.

These points are fitted by a straight line and their dispersion around this line is less than 2.5 %. This confirms that there is no saturation effect in these APDs.

However, to be sure this effect was not due to the heating of the LED itself, this is placed at 20 cm from the APD and the light is conducted by an optical fibre. The results of the measurements show the same effect as previously.

The stability of the blue LED has been also checked by a PIN diode. The variation of the LED intensity over 5 mn is below 0.5% with the dc forward current reaching 50 mA.

In order to avoid these problems, all following measurements are made with a dc forward current of blue LED close to 0.5 mA.

4.3 Gain measurements

Figure 5 shows the measured APD photocurrent exposed to the blue LED versus bias voltage. The temperature for these measurements is stable and around $24.5 \pm 0.5°C$.

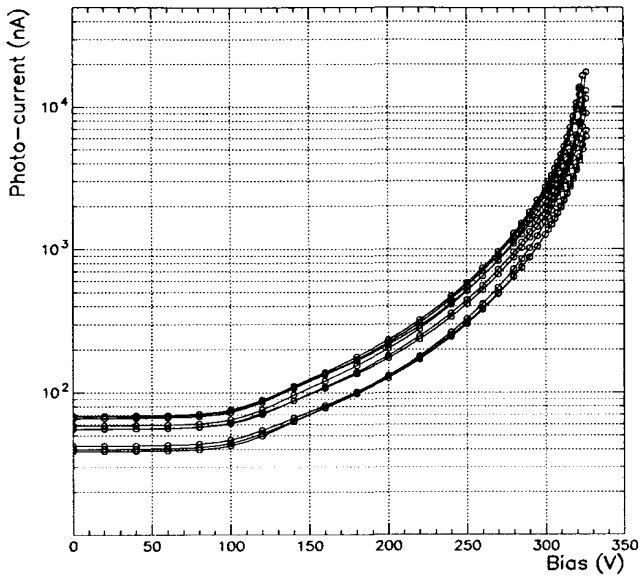

Figure 5: Photocurrent of Hamamatsu APDs, exposed to the blue LED, versus bias.

In the range of 0 to 70 V biases the value of the photocurrent is constant and corresponds to the conditions where the multiplication does not exist and the APD works like an ordinary PIN photodiode. Above 70 V the multiplication process starts and the photocurrent rises when we approach the breakdown conditions at approximately 330 V. The constant behaviour of the photocurrent, with biases from 0 to 70 V, gives a good estimate of the range of biases where the gain is equal to 1.

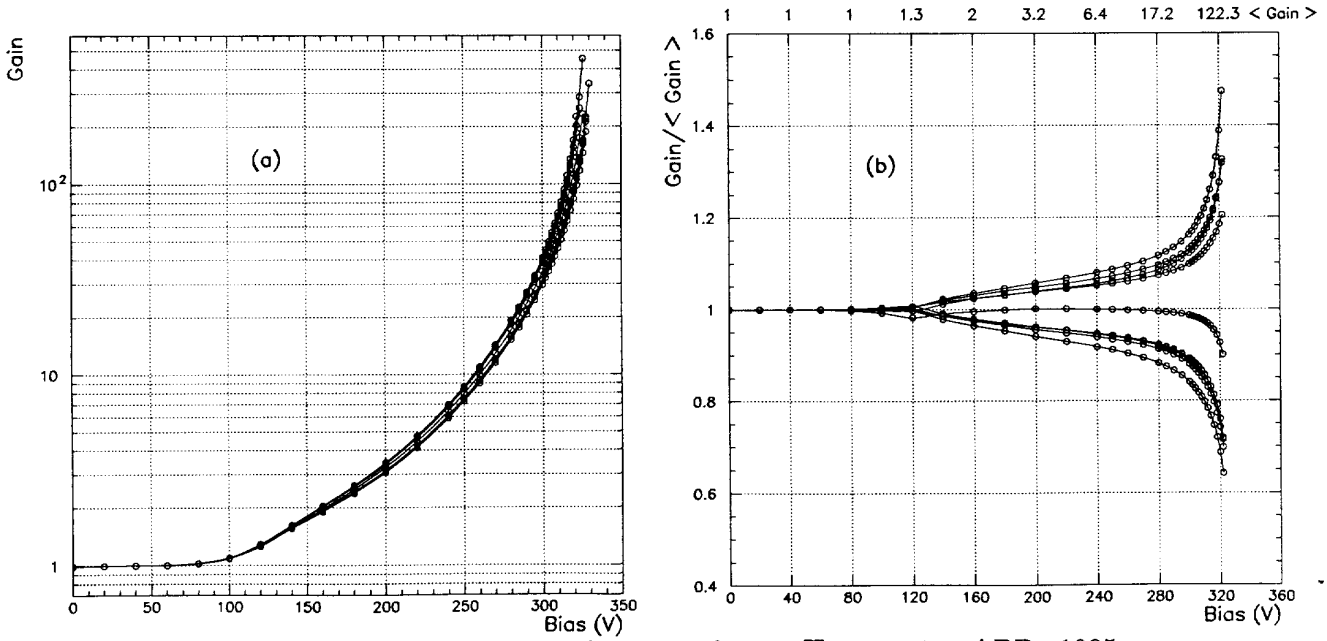

Figure 6: Gain measurements for nine low capacitance Hamamatsu APDs 1995.

The photocurrent measurements are normalised with the value of the photocurrent recorded at bias 40 V which corresponds to a unitary gain. The results are plotted in figure 6 (a).

Figure 6 (b) shows the gain of APDs normalised to the mean value of APD gain calculated from the nine Hamamatsu APD gains. The dispersion of the gain measurements is smaller than 10% for a bias below 260 V while at high voltage it increases exponentially and reaches 50% at a gain of 120. This large dispersion above 300 V is due to the photocurrent of the APDs which seems to increase differently as a function of bias as shown in figure 5. Thus, for example, at bias 310 V the gain mean value is around 58 with an R.M.S. of 9.

4.4 Gain variation as a function of bias

From our previous gain measurements, we can estimate the sensitivity of the gain to the variation of the APD bias voltage. This sensitivity is defined by the formula:

$$\frac{1}{G}\frac{\Delta G}{\Delta V}\ (\%/V) = \frac{2}{G_2+G_1}\ \frac{G_2-G_1}{V_2-V_1} \times 100$$

where G_1 and G_2 are respectively the gain measured at bias V_2 and V_1. The obtained results for nine APDs as a function of the gain value are identical as shown in figure 7.

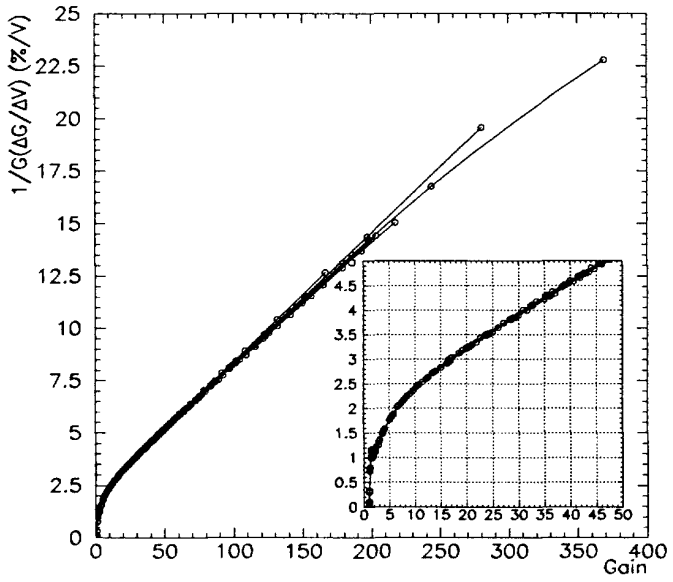

Figure 7: Sensitivity of the gain of the nine APDs to the bias as a function of the gain value.

It seems that the gain sensitivity to the bias is the same for all APD. From these curves, we approximately deduce the analytic formula:

$$\frac{1}{G}\frac{\Delta G}{\Delta V}\ (/V) \simeq 0.02 + 6\ 10^{-4} G$$

with $G > 10$

Thus we expect, for example, a variation of 5% per volt at a gain of 50.

4.5 Gain variation as a function of temperature

We have performed gain measurements for five APDs at $21°C$ and $24.5°C$ over the whole range of bias. The stability of the temperature is at $0.5°C$. This is not sufficient to measure precisely the gain sensitivity to the temperature. Therefore the following results are to be taken with care. The gain variation as a function of temperature is estimated in this way:

$$\frac{1}{G}\frac{\Delta G}{\Delta T}\ (\%/°C) = \frac{2}{G_2+G_1}\frac{G_2-G_1}{T_2-T_1} \times 100$$

where G_1 and G_2 are respectively the gain measured at temperature T_2 and T_1. The results are presented in figure 8 as a function of the gain of the APD.

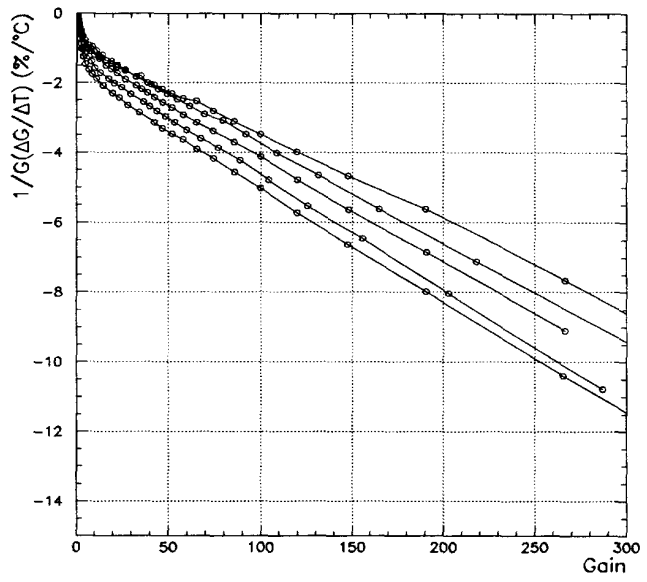

Figure 8: Sensitivity of the gain APD to temperature as a function of the gain value.

With a gain value greater than 10, the behaviour of $\frac{1}{G}\frac{\Delta G}{\Delta T}$ is linear but the slopes look slightly different from one APD to another. For example, at gain 50, the $\frac{1}{G}\frac{\Delta G}{\Delta T}$ varies between 2.5 and $3.5\%/°C$.

4.6 Bulk leakage current measurements

Knowing the gain and the dark current values for each APD, it is possible to measure the bulk leakage current I_b by measuring the I_d/G ratio at high gain.
Indeed we have:

$$\frac{I_d}{G} = \frac{I_s}{G} + I_b$$

and at high gain, $G > 50$,

$$\frac{I_d}{G} \simeq I_b$$

Figure 9 shows Id/G as a function of the gain for each APD.

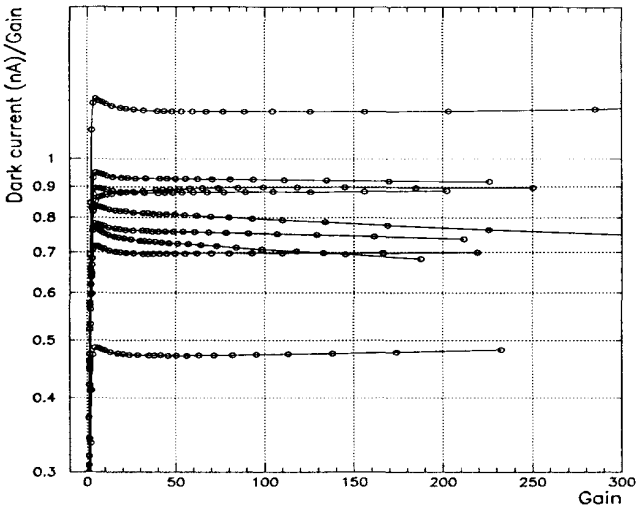

Figure 9: The Id/G of Hamamatsu APD 1995 at temperature of $24.5°C$.

Above a gain of 20 this ratio becomes stable and can be identified as the bulk leakage current I_b. The mean value of the bulk leakage current, computed from these curves, is 0.8 nA with an R.M.S. of 0.19 nA.

4.7 Bulk current variation as a function of temperature

We have also recorded the variation of the bulk leakage current as a function of temperature for several APDs. Figure 10 shows the results obtained at three values of temperature for the APD having the lowest dark current.

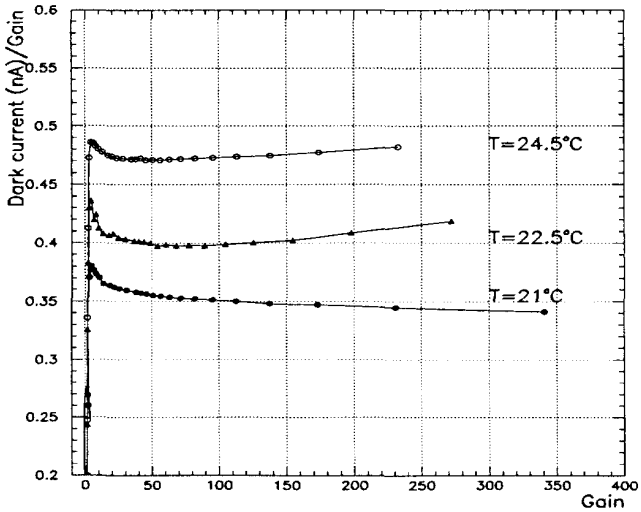

Figure 10: The Id/G of one Hamamatsu APD 1995 for three values of temperature.

By extrapolating these measurements we expect the bulk current to rise by a factor of 80 to 110% when the temperature increases by $10°C$. This is compatible with what we know from the Si diode inverse current [6]. Notice that the same measurements have been done for four other APDs and they have given a similar result.

5 Pulsed light method

5.1 Experimental set-up

Two other methods based on the pulsed light and gamma sources are used to measure the gain of the APDs. These APDs are associated to a L3 charge preamplifier [5] with a satisfactory linearity. The signal is then sent to a RC-CR^n shaping amplifier [3] with a fixed shaping time of 0.5 μs. This method, using a charge preamplifier and slow shaping is less sensitive to the shape of light pulse. Figure 11 shows a schematic view of the experimental set-up.

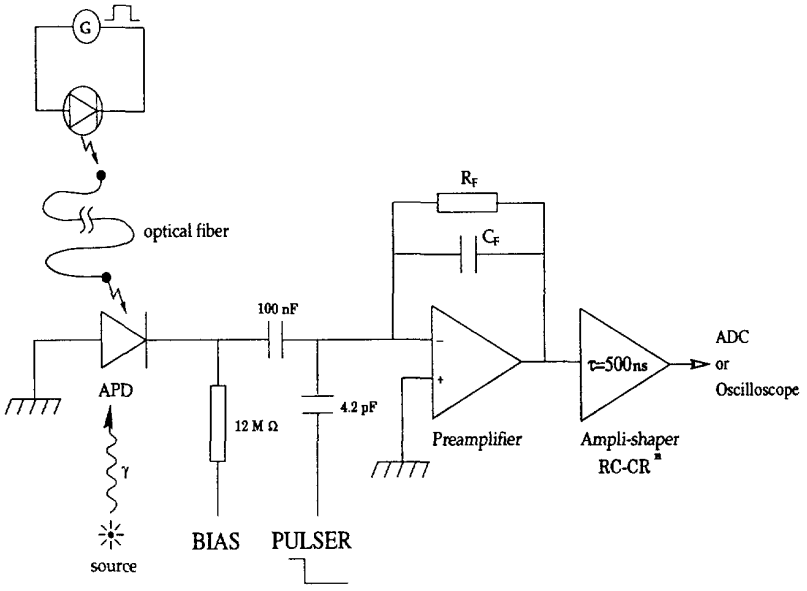

Figure 11: Experimental set-up

The polarisation tension of the APD is set by the Keithley 487/source voltage through a load resistance (R=12 MΩ) and therefore the true bias seen by the APD is given by:

$$V_{APD} = V_{Keithley} - R\ I_d$$

where I_d is the dark current dependent on the bias V_{APD} on APD.

5.2 Time response of APD

In a recent RAL report [7] some waveforms of the EG&G APD response, irradiated by 5.9 keV X-rays, have been recorded. The authors found that these waveforms were not ballistic pulses.

[3]ORTEC 572

In the case of our nine low capacitance Hamamatsu APDs exposed to the 5.9 keV gamma from ^{55}Fe source, the waveform responses are similar to a ballistic pulse. Figure 12 shows an example of a typical response of the APDs at γ excitation. The rise time of our charge preamplifier is around 10 ns for a detector capacitance of 100 pF.

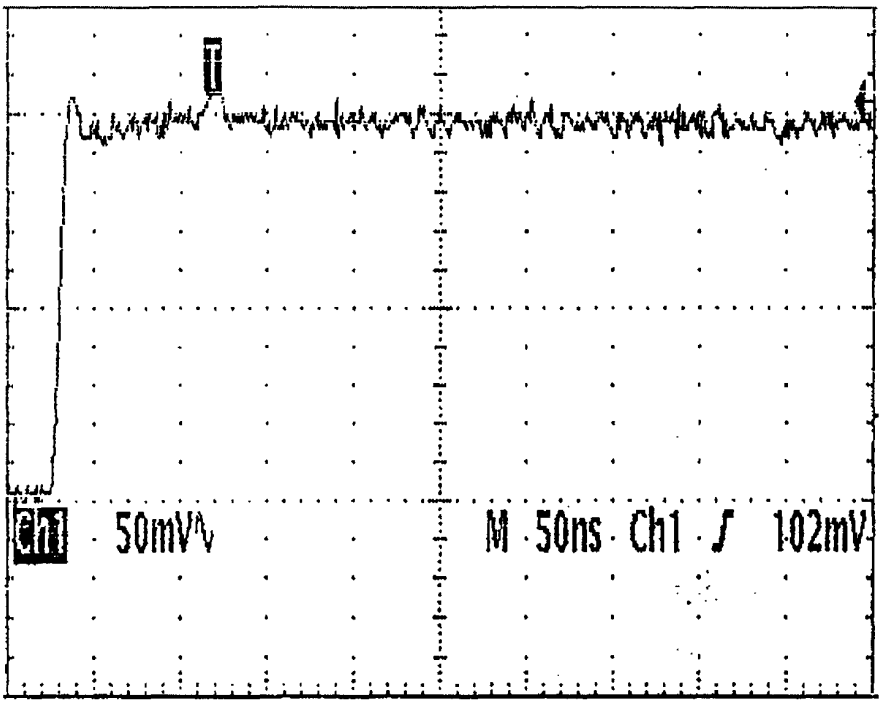

Figure 12: A single shot oscilloscope trace of a " 5.9 keV ^{55}Fe gamma" induced pulse in an Hamamatsu APD.

5.3 Gain measurements with pulsed light and gamma sources

Two other methods were used to measure the gain of APDs:

- **pulsed light:** The pulsed light is produced by a blue LED driven by a pulse generator of 50 Hz. The gain is defined as the pulse height measured at the end of the electronics chain for a given bias normalised to the pulse height measured at 40 V bias.

- **gamma source:** We have used the same setup with a gamma source instead of a pulsed light and with a peak sensing ADC [4] instead of a oscilloscope. The calibration factor in the electron charge (k) of this ADC and the pedestal are estimated with a pulser and a known calibration capacitance of 4.2 pF as shown in figure 11. Thus the gain is given by the following formula:

$$G = (ADC\ channel - pedestal\ channel) \times k \times \frac{3.62eV}{E_\gamma}$$

where E_γ is the energy of the photon emitted by the source and 3.62 eV is the mean energy necessary to create an electron-hole pair in the silicon. The error on the gain value is 4% due to the uncertainty on the calibration capacitance value.

[4]Nucleus PC board (13 bits ADC)

Typical spectra of ^{241}Am and ^{55}Fe are shown in figure 13 with the peaks corresponding to the main gamma rays. The width of these peaks is due essentially to the electronic noise. These spectra are obtained with the APD bias of 260 V in the case of the ^{241}Am source and 300 V in the case of the ^{55}Fe source.

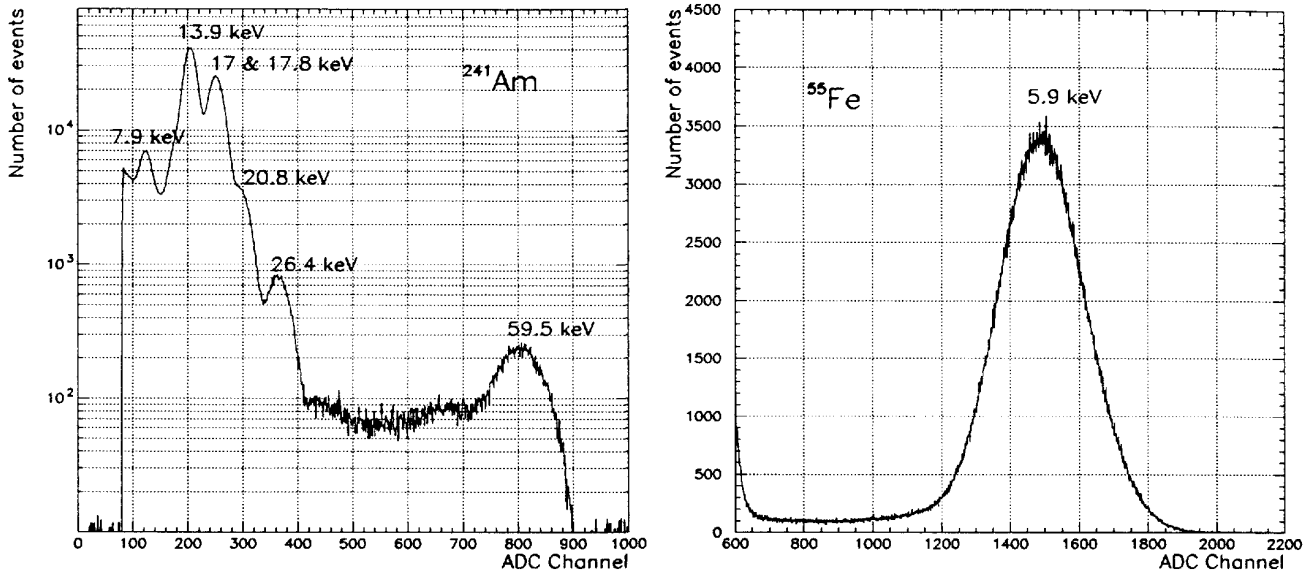

Figure 13: ^{241}Am and ^{55}Fe spectra.

Figure 14 presents the gain measurements obtained using the ^{55}Fe and the ^{241}Am gamma sources. These new measurements are compared to the results obtained with a continuous light source and show a difference at high gain.

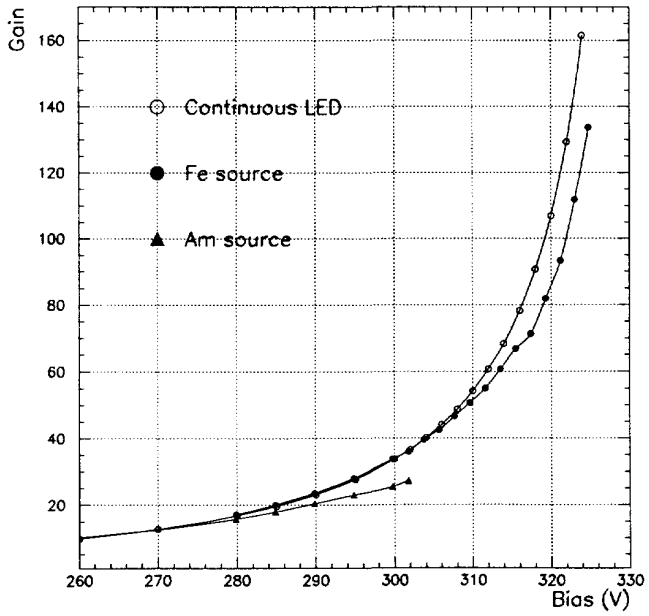

Figure 14: Gain values measured with the ^{55}Fe and ^{241}Am gamma sources compared with the continuous light measurements.

At low gain the results obtained by the gamma source method are in agreement with the continuous light results while at high gain they are lower by a factor of 25%.

We can explain this effect by a saturation of the multiplication process due to the "screening effect" in the case of high density of charge created in avalanche region [3]. This saturation depends also on the total charge created by the gamma. Indeed, the slope of the 59 keV ^{241}Am X-ray curve is flatter than that of the 5.9 keV ^{55}Fe X-ray curve as shown in figure 14.

We have also compared the gain measurements performed by the pulsed light method to the continuous light method as shown in figure 15.

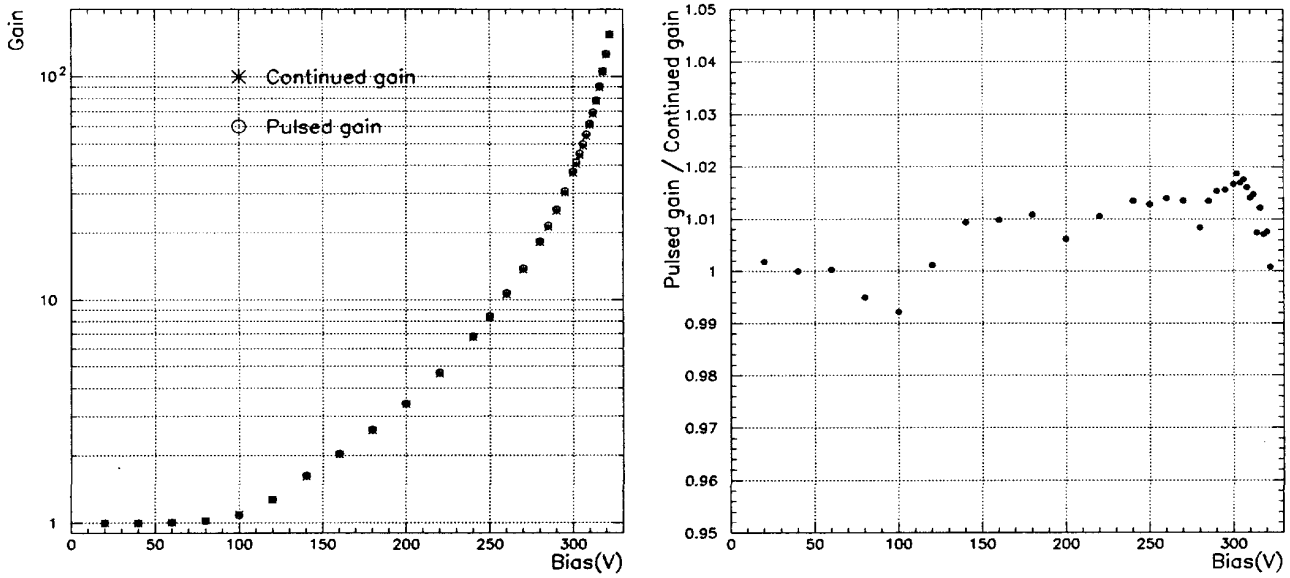

Figure 15: Gain values measured with the pulsed light compared with the continuous light measurements.

The difference between the results given by these two methods is less than 2% over the full range of bias.

5.4 Equivalent noise charge

Theoretically, the equivalent noise charge of the APD, in electrons, associated to a JFET preamplifier followed by a RC-CR amplifier is given by [8]:

$$ENC^2 \approx \frac{e^2}{8q^2}\left[2q(I_s + G^2 I_b F)\tau + 4k_B T\left(R_s\left(\frac{C_D}{C_T}\right)^2 + \frac{0.7}{g_m}\right)C_T^2\frac{1}{\tau}\right] \qquad (1)$$

where:

- I_b and I_s: bulk and surface leakage current of the APD respectively.
- C_D and R_s: capacitance and serial resistance of APD respectively.
- $C_T = C_D + C_{in}$ where C_{in} is the input capacitance of the preamplifier.

- F: excess noise factor of the APD.
- τ: shaping time of RC-CR amplifier. In our experiment it has a value of 0.5 μs.
- q, k_B and gm: electric charge, Boltzmann constant and transconductance value of the preamplifier respectively.

The 1/F noise term has been neglected in the previous formula.

The ENC measurements have been done with different APD gain values by using an ORTEC 448 research pulser. Indeed a finite charge, given by a pulser, is sent to the input of the preamplifier. The width of the peak is recorded and converted into electrons by the calibration coefficient k defined in the previous section.

The ratio of the electronic noise to the APD gain versus gain is shown in figure 16.

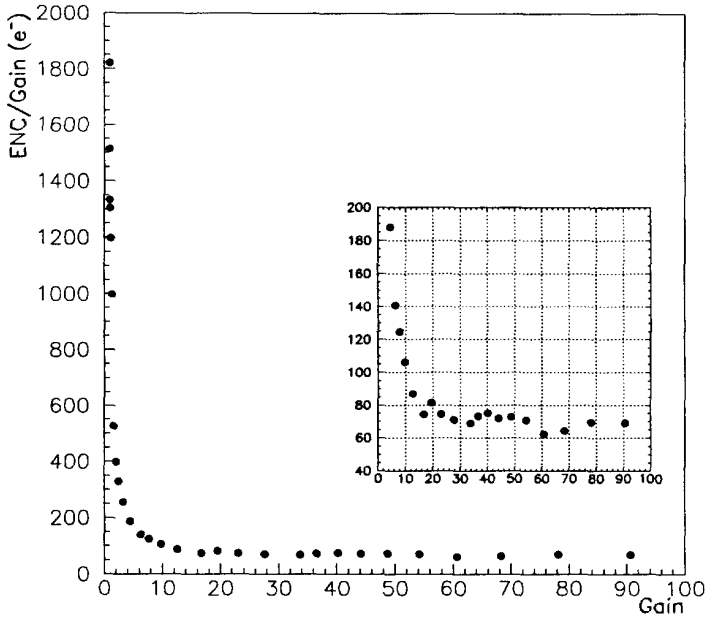

Figure 16: Equivalent noise charge/gain ratio versus gain.

As at very low gain the APD is not fully depleted, the contribution of the APD capacitance term to the ENC dominates as we can see in figure 16.

At high gain equation (1) becomes:

$$\left(\frac{ENC}{G}\right)^2 = \alpha I_b F \tau \tag{2}$$

where we only have the simultaneous contribution of the excess noise factor and the bulk leakage current. As we have used in this set-up an RC-CR^n amplifier the value of α constant is somewhere between 1.2 and 1.5.

Figure 16 shows that the curve is almost stable for gains above 30 and the ratio reaches a minimum of 70 electrons. As the bulk current is constant in this region (see section 4.6), this suggests that the excess noise factor depends weakly on the gain value. From equation 2 we have approximately estimated the excess noise factor to two limit α values: 1.2 and 1.5. With this assumption on α, the F value varies between 1.9 and 2.2.

5.5 Excess noise factor

Once a satisfactory electronic noise charge is reached, we have used the same set-up to measure the excess noise factor of the previous APD for three values of bias. The method used was already explained in the technical note [3]. Briefly, the way to measure F is to use the fluctuations of the pulsed light amplitude σ_t. Indeed we have:

$$\left(\frac{\sigma_t}{A_t}\right)^2 = \frac{F}{N_{pr}} + \left(\frac{\sigma_n}{A_n}\right)^2 + \left(\frac{\sigma_{st}}{A_{st}}\right)^2$$

where σ_n is the electronic noise corresponding to the width of the peak pulser. The signal amplitude given by a pulser, A_n, is adjusted to the amplitude given by the LED A_t in order to avoid a possible problem of non linearity of the preamplifier.

In order to estimate the LED stability $\frac{\sigma_{st}}{A_{st}}$, we have exposed a PIN diode [5] to the pulsed LED of a duration of 30. As F equals 1 in this case, the results obtained suggest that the stability is better than 0.5%.

For the following measurements the LED pulse duration is set to 10 ns with a cycle time of 20 ms. The LED stability term $\frac{\sigma_{st}}{A_{st}}$ is neglected in the next calculations since this value is added quadratically.

The number of primary photoelectrons N_{pr} created before the avalanche region is estimated in two ways:

- Knowing the calibration of the peak sensing ADC and the gain of APD (see section 4.3) we can estimate the number of photoelectrons by:

  $$N_{pr} = (A_t - pedestal) \times k \times \frac{1}{G}$$

  This method assumes a good precision on the gain value.

- The aim of the second method is to avoid the use of the gain value thus eliminating the contribution of its uncertainty. For this we have measured the signal amplitude of LED with an APD under a bias of 50 V. At this bias the APD works like a photodiode with a gain equal to 1. Unfortunately, the signal is very close to the pedestal. To overcome this problem we have proceeded in this manner:

  1. At a bias of 50 V we have increased the pulse duration of LED until the signal became visible. This corresponds to a pulse duration of 60 ns.
  2. We have then chosen a bias of APD corresponding to a given value of a gain. In our case the bias is set to 220 V corresponding to a gain around 4. Two measurements are done at a pulse duration of 10 and 60 ns. From these measurements we deduce the increase factor of the photoelectrons when we go from a 10 to 60 ns pulse duration.

  At the end of the procedure the number of photoelectrons measured at bias 50 V with a pulse duration of 60 ns is normalised by the previous factor to obtain the number of photoelectrons with a duration pulse of 10 ns.

[5] Hamamatsu S3590-01 of 70 pF capacitance and a bulk leakage current around 0.5 nA

Table 1 shows the excess noise factor F measured for three values of gain with the two methods. F seems to depend weakly on the gain.

Bias (V)	Gain	Excess noise factor	
		method 1	method 2
290	23	1.90	1.82
304	40	2.03	1.95
318	91	2.43	2.36

Table 1: Excess noise factor

The difference between the results obtained by the two methods is less than 4%.

6 Conclusion

Some characteristics of nine Hamamatsu APDs have been investigated. We have observed, at a reasonable gain (G <50) measured by the continuous light method, a small dispersion on the gain value (figure 6). In this range the sensitivity of the gain to temperature and bias is less than 3.5% (figure 7) and 5% (figure 8) respectively.

At high bias an important dispersion in the gain value between the APDs is observed and the sensitivity of the gain to temperature and bias is enhanced.

The gain measurements are obtained for each APD by the following three methods: a gamma source, pulsed and continuous light, which are compared. Each shows an agreement at low bias equivalent to low gain. At high gain the gamma source measurements are lower by approximately 20% in comparison with the continuous light results while the pulsed light measurements still remain in agreement.

Acknowledgements

We thank G. Maurelli and P. Sahuc for their technical help.

References

[1] "Compact Muon Solenoid Technical Proposal", CERN/LHCC 94-38 (1994)

[2] M. Goyot, "Development of high speed low noise transimpedance preamplifier in bipolar technology for silicon photodetectors of the CMS electromagnetic calorimeter", Talk given at "The first Workshop on Electronics for LHC Experiments", Lisbon, 11-15 September 1995

[3] A. Karar et al., "Investigation of Avalanche Photodiodes for EM Calorimeter at LHC", CMS-TN/95-095

[4] Hewlett Packard, "SiC Blue T-1 3/4 LED Lamps", RS 257-22384 DB15

[5] M. Goyot et al., "Performances of a preamplifier silicon photodiode readout system associated with the large BGO crystal scintillators", NIM A263 (1988) 180

[6] E. Gramsch et al., "The avalanche photodiode catalog", Advanced Photonix Inc

[7] J.E. Bateman and R. Stephenson, "Charge storage effects in some avalanche photodiodes proposed for use in the CMS ECAL", RAL-TR-95-000

[8] E. Gatti et P.E. Manfredi, "Processing the signals from solid-state detectors in elementary particle physics", La Rivista del Nuovo Cimento, Vol. 9, N. 1, 1986